Electronic Supplementary Material (ESI) for Analytical Methods.
This journal is © The Royal Society of Chemistry 2019

Supplementary information

# Hydrogen peroxide detection with a silver nanoparticle grating chip fabricated by plasmonic plating

Hiroyuki Yoshikawa,* Kenshiro Hieda, Kanako Ikeda and Eiichi Tamiya
Department of Applied Physics, Osaka University, Suita, Osaka 565-0871, Japan
E-mail: yosikawa@ap.eng.osaka-u.ac.jp

## Scanning electron microscope (SEM) measurement

The surface nanostructure of an AgNP grating chip (Figure 1d) was measured by SEM (DB235, FEI). Figure S1 shows a SEM image around a dark green line of the grating structure. Silver nanoparticles of size 30–70 nm are observed near the center of the line. Smaller nanoparticles to both the left and right of the image are gold nanoparticles on the glass substrate, which correspond to the bright lines in Figure 1d.

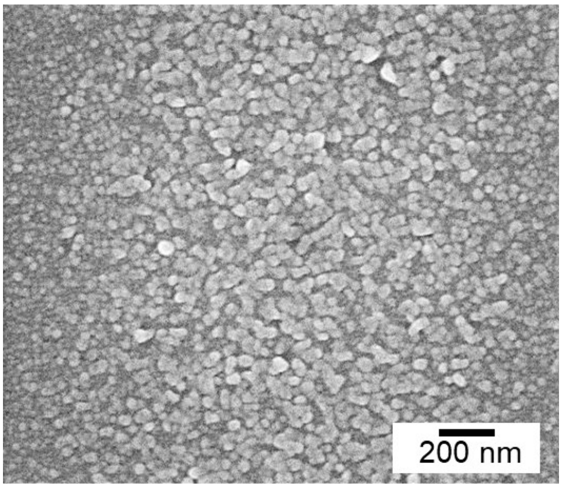

**Fig. S1** SEM image of AgNP grating chip surface.

## Simulation procedure of diffraction efficiency vs. thickness of an AgNP assembly layer

The diffraction efficiency of an AgNP grating chip was calculated based on the Rigorous Coupled-Wave Analysis (RCWA) method, as shown in Figure 3. The periodic line structures on the chip are composed of AgNP assemblies, whose complex refractive index (RI) is unknown. In this study, the RI was estimated from the ellipsometry analysis. To perform this analysis, AgNP assemblies were deposited in a few centimeter-wide spots on a glass substrate by plasmonic plating with LED irradiation, as reported in a previous paper.[1] This substrate was set on an ellipsometer (M2000, J.A.Woollam), and the difference in phase shift (Δ) and the ratio of amplitude change (Ψ) were measured as a function of the wavelength of light, as shown in Figure S2. The complex refractive index at each wavelength was calculated from the Δ and Ψ spectra by employing analysis software attached to the ellipsometer (Figure S3).

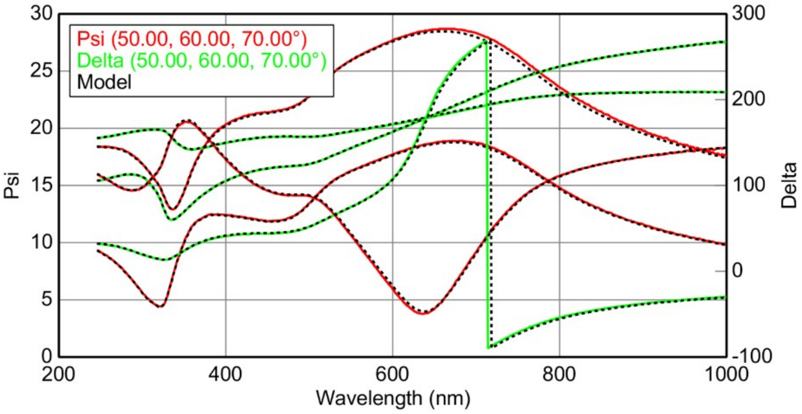

**Figure S2** Spectroscopic ellipsometry data of an AgNP assembly layer fabricated by plasmonic plating (red: amplitude change, green: phase shift, dotted: curve fitting data) measured at three incident angles (50°, 60°, and 70°).

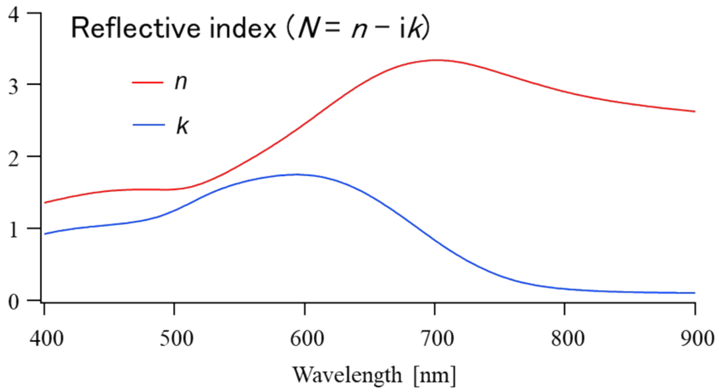

**Figure S3** Complex refractive index of AgNP assembly layer calculated from ellipsometric data in Fig. S1.

The RCWA simulation was performed by the DiffractMOD software (Rsoft), which considers a 2D simulation model of rectangular AgNP assemblies periodically arranged on a glass plate. The interval of this grating structure was set to be the same as that of the real chip. The incident laser wavelength and incident angle were also set to be the same as experimental conditions. The first order diffraction efficiency was calculated for each thickness of the AgNP assembly layer (0–15 nm, step size = 0.5 nm).

### Simulation for AgNP grating chips with different grating periods

Similar RCWA calculations were performed for grating chips with different grating periods. As shown in Figure S4, the sensitivity (the slope of the AgNP layer thickness vs diffraction efficiency) of the 1 μm grating period increases by a few tens of %. However an optical setup for the interference exposure becomes difficult to construct, because two laser beams must be overlapped at a large angle to fabricate such a short-period grating. In addition, the contrast of the grating structure becomes worth because the accuracy of the fabrication is limited by the optical diffraction limit. For these reasons, we decided the grating period to 1.8 μm in this work.

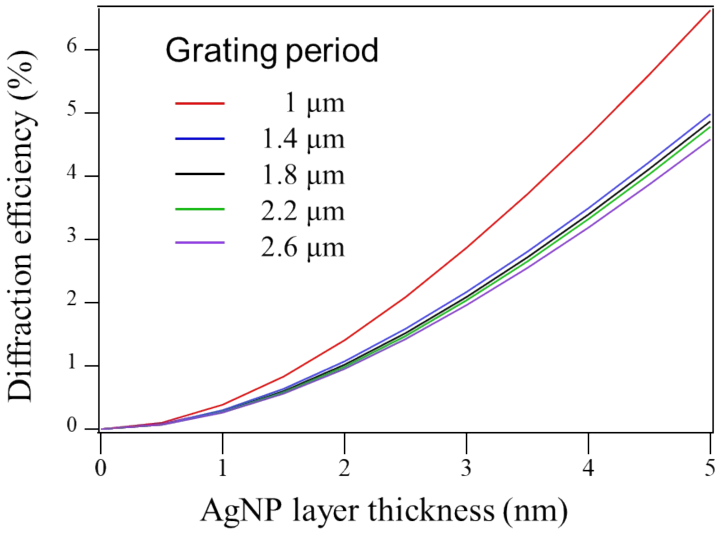

**Figure S4** Calculation result of diffraction efficiency of grating chips with different grating periods.

### pH dependence of the $H_2O_2$ detection

The $H_2O_2$ detections were performed at pH 4 (50 mM ascorbate buffer) and pH 9 (10 mM borate buffer) as shown in Fig. S5. Temporal changes of the diffraction intensity are small and barely dependent on the $H_2O_2$ concentration at pH 4. At pH 9, higher $H_2O_2$ concentrations decrease diffraction intensities in a shorter time as shown in Fig. S5b, but the degree of the intensity change (score value) is smaller than that measured in aqueous solution. We estimated that limit of detections at pH 4 and pH 9 are > 334 μM and > 13.4 μM, respectively. D. He et al. investigated the decomposition of colloidal AgNPs in 10 mM $H_2O_2$ solution at different pH conditions by measuring the optical absorbance of the AgNP plasmon band. [2] They also reported that the AgNP absorbance decreases rapidly at pH 7 as compared to that at higher or lower pH conditions. The mechanism of the pH dependence related to superoxide anion is deeply discussed in the previous study. [2]

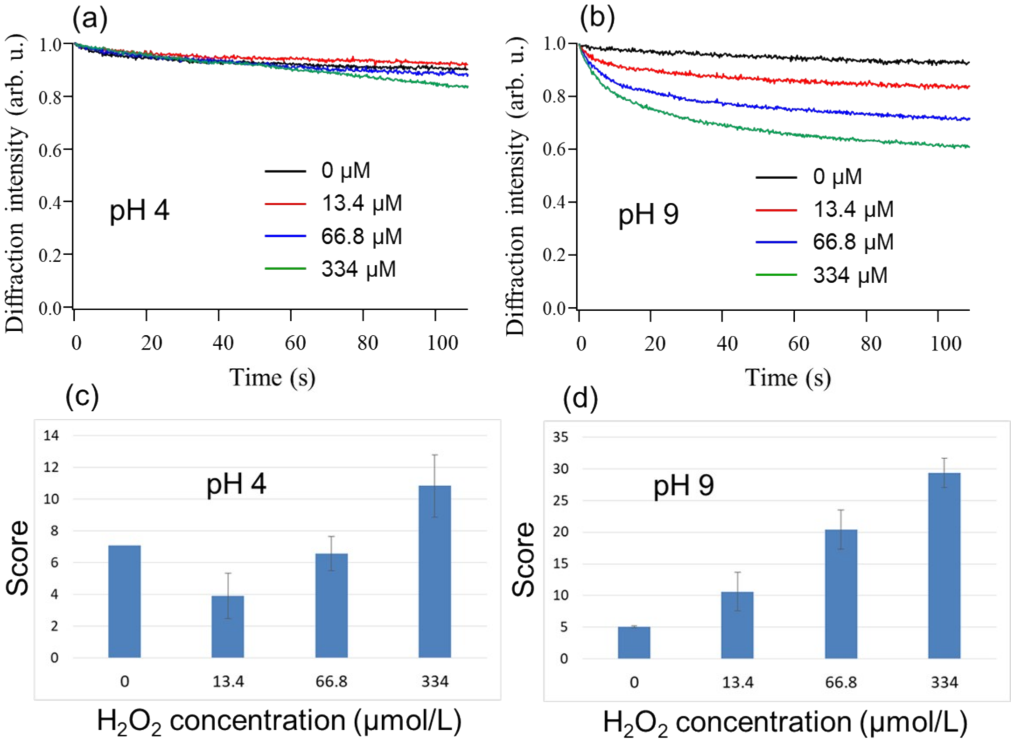

**Figure S5** Temporal changes of diffraction intensities (a, b) and score values (c, d) measured at pH 4 (a, c) and pH 9 (b, d).

## SEM and absorption spectrum analyses of AgNP grating chips before and after the $H_2O_2$ detection

AgNP grating surfaces were analyzed by SEM and energy dispersive X-ray spectrometry (EDX) before and after the $H_2O_2$ detection. This analysis was performed by S-5200 (Hitachi). Fig. S6a shows a SEM image of a grating structure fabricated by 5-min laser exposure. A grating structure is clearly observed before $H_2O_2$ detection. Bright lines are composed of dense AgNPs assembly (Fig. S6b). After the application of $H_2O_2$ solution (30 mM) for 3 min, the grating structure becomes unclear and larger particles are formed (Fig. S6d). The particle density is much lower than that before the $H_2O_2$ detection and AuNPs are exposed between particles (Fig. S6e). These results indicate that the periodic structures composed of densely-deposited AgNPs are decomposed by $H_2O_2$ and the decrease of the periodic contrast diminishes the diffraction intensity. Large particles produced after the $H_2O_2$ detection may be reproduced AgNPs. D. He et al. reported that superoxide anions, which are produced by the interaction between $H_2O_2$ and AgNPs, mediates reduction of Ag ions and reformation of AgNPs. [2] Fig. S6c and S6f show EDX spectra of Fig. S6b and S6e, respectively. After the $H_2O_2$ detection, the relative peak intensity of Ag still remains, suggesting the reformation of AgNPs.

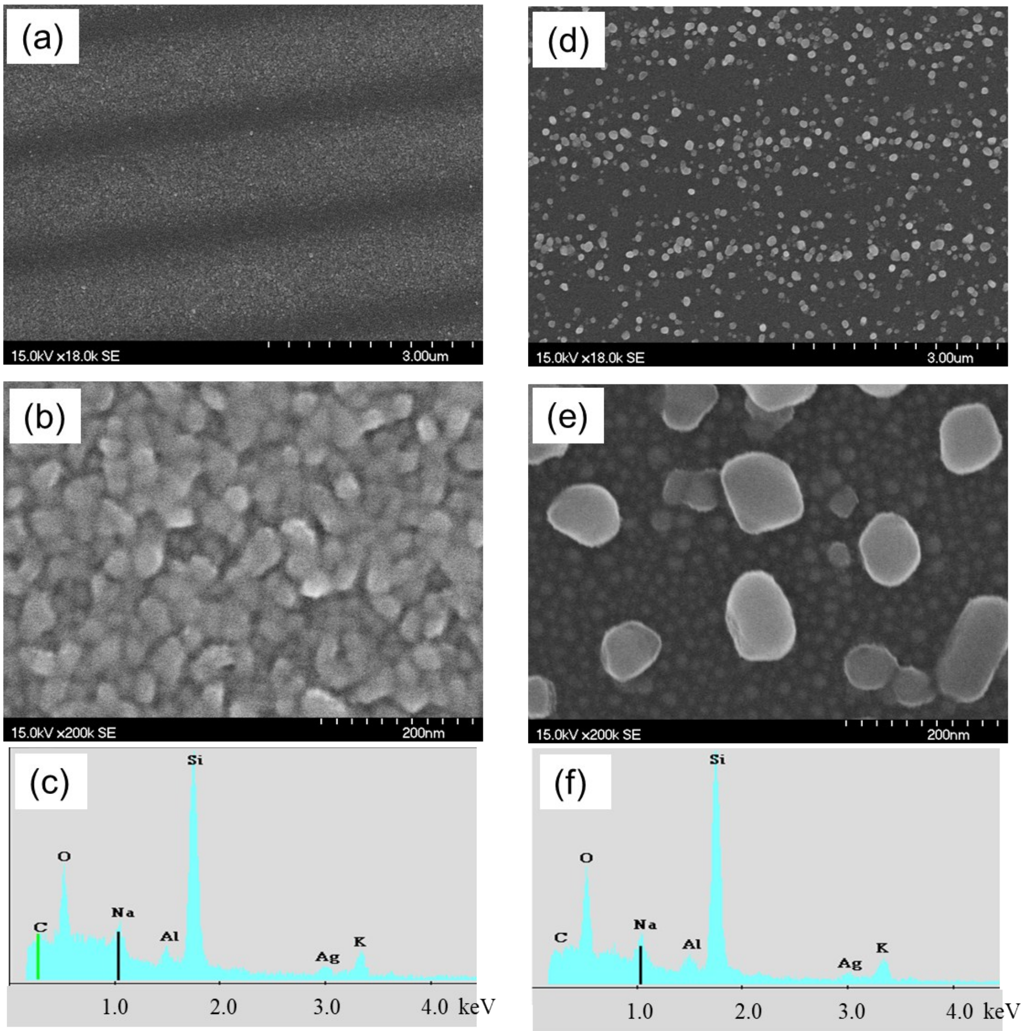

**Fig. S6** SEM images of AgNP grating chips before (a, b) and after (d, e) the $H_2O_2$ detection. (c, f) EDX spectra of surface areas represented (b) and (e), respectively.

An absorption spectrum of the AuNP substrate showed a plasmon band at 532 nm (Fig. S7, black line). For the fabrication of grating sensor chip, AgNPs were deposited on the AuNP substrate by plasmonic plating method combined with an interference laser exposure for 10 s. An increase in absorbance and a red-shift of the peak wavelength to 540 nm were shown due to the AgNP deposition (red line). After the $H_2O_2$ detection (334 μM), the absorbance decreased and the peak wavelength showed a blue-shifted to 531 nm (blue line), which was close to the plasmon band of the original AuNP substrate. These spectral changes demonstrate the decomposition of AgNPs by the $H_2O_2$ detection.

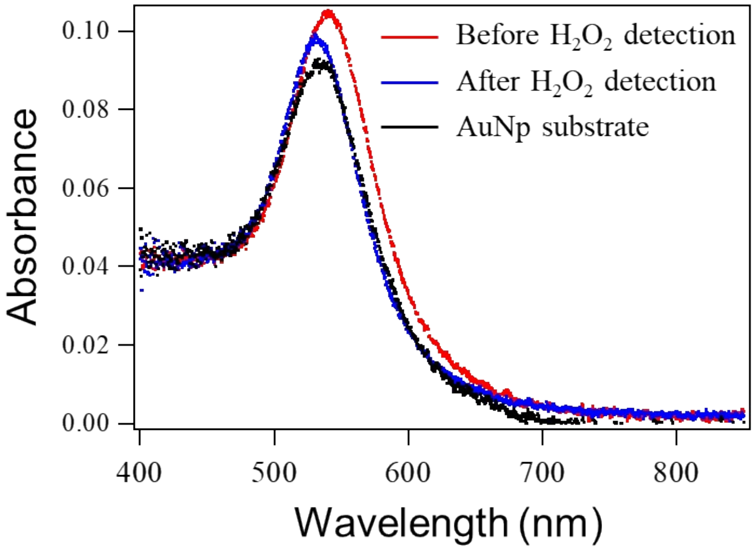

**Figure S7** Absorption spectra of an AuNP substrate (black) and AgNP grating chips before (red) and after (blue) the $H_2O_2$ detection

**Reference**

1) H. Yoshikawa, A. Hironou, Z. J. Shen and E. Tamiya, *ACS Appl. Mater. Interfaces*, 2016, **8**, 23932 –23940.

2) D. He, S. Garg and T. D. Waite, *Langmuir*, 2012, **28**, 10266-10275.